Available online at www.sciencedirect.com
SCIENCE DIRECT
Polymer 46 (2005) 9965–9973
polymer
www.elsevier.com/locate/polymer

Viscoelastic properties and morphological characterization of silica/polystyrene nanocomposites synthesized by nitroxide-mediated polymerization

Christèle Bartholome[a,b], Emmanuel Beyou[a,*], Elodie Bourgeat-Lami[b], Philippe Cassagnau[a], Philippe Chaumont[a], Laurent David[a], Nathalie Zydowicz[a]

[a]*Laboratoire des Matériaux Polymères et des Biomatériaux, UMR CNRS 5627, Université Claude Bernard-Lyon 1. Bât. ISTIL. 43 Bd. du 11 Novembre 1918, 69622 Villeurbanne Cedex, France*
[b]*Laboratoire de Chimie et Procédés de Polymérisation. CPE. Bât. 308F. BP 2077. 43, Bd. du 11 Novembre 1918, 69616 Villeurbanne cedex, France*

Received 10 November 2004; received in revised form 24 June 2005; accepted 19 July 2005
Available online 6 September 2005

Abstract

Polystyrene (PS) chains with molecular weights comprised between 15,000 and 60,000 g/mol and narrow polydispersities were successfully grown from the surface of silica nanoparticles by nitroxide-mediated polymerization (NMP). Small angle X-ray scattering was used to characterize the structure of the interface layer formed around the silica particles, and at a larger scale, dynamic light scattering was used to determine the hydrodynamic diameter of the functionalized silica suspension. In a second part, blends of PS-grafted silica particles and pure polystyrene were prepared to evaluate the influence of the length of the grafted PS segments on the viscoelastic behavior of the so-produced nanocomposites in the linear viscoelasticity domain.

Combination of all these techniques shows that the morphology of the nanocomposite materials is controlled by grafting. The steric hindrance generated by the grafted polymer chains enables partial destruction of the agglomerates that compose the original silica particles when the latter are dispersed either in a solvent or in a polymeric matrix.

Keywords: Polystyrene-grafted silica gel; Morphology; Viscoelastic

1. Introduction

A key point in the development of nanostructured materials is the research of specific interactions at the interface of the organic and inorganic components. Among the large palette of existing techniques, living polymerizations offer versatile ways to engineer inorganic particle surfaces. Controlled radical polymerization has been used to build up highly dense polymer brushes from planar surfaces [1], and was recently extrapolated to nanoparticles functionalization in order to elaborate well-defined nanocomposites which can be grown with the desired thickness and composition [2–10]. We have shown in a previous paper [9] that polystyrene (PS) chains with molecular weights comprised between 15,000 and 60,000 g/mol and narrow polydispersities can be successfully grown from the surface of silica nanoparticles through nitroxide mediated polymerization (NMP). The maximum grafting density of the surface-tethered PS chains was estimated to be around 0.35 μmol/m^2 and seemed to be limited by initiator confinement at the interface.

In order to study the surface organization of such nanocomposite systems, and more precisely to determine the influence of the length of the PS segments on the composite nanostructure, small angle X-ray scattering was used to characterize the nanostructure at the scale of the primary silica particles and the width of the interface polymer layer, while at a larger scale, dynamic light scattering and transmission electron microscopy were used to determine the hydrodynamic diameter of the functionalized silica particles and characterize the overall dispersion state of silica. Since the chain length of the grafted

* Corresponding author.
E-mail address: beyou@univ-lyonl.fr (E. Beyou).

0032-3861/$ - see front matter © 2005 Elsevier Ltd. All rights reserved.
doi:10.1016/j.polymer.2005.07.057

polystyrene can be accurately controlled by the NMP technique, the nanocomposite morphology could be in principle monitored by simply changing the polymer molecular weight.

In a second part, we characterized the viscoelastic behavior in the linear viscoelasticity domain of nanocomposite materials obtained by dispersing the grafted silica particles into a polystyrene matrix. Such experiments are expected to provide information on chain dynamics and silica particles dispersion state via the temperature and frequency variations of the complex shear modulus $G^*(\omega)$. It has already been pointed out by Dagreou et al. [11] that rheology is, to this respect, a powerful tool from both an experimental and a theoretical point of view. Based on this approach, a new theoretical network model on the viscoelastic behavior of non-entangled polymer melts reinforced with well dispersed non-agglomerated particles has been recently presented [12]. However, this previous work was carried out on colloidal silica particles whereas the silica used in the present study is a fumed silica. Since the nature of the silica particles is known to significantly influence the final properties of the materials, we can expect to observe in the present work different behaviors than those described previously.

In summary, this paper deals with the morphological characterization and viscoelastic properties of nanocomposite materials made of polystyrene-grafted silica particles dispersed in a polymer matrix. The polymer chain lengths (M_n ranging from 15,000 to 60,000 g/mol) and grafting densities were varied in a large range in order to investigate the effect of these two parameters on the composite nanostructure.

2. Experimental section

2.1. Stable free radical polymerization of styrene from the functionalized silica surface

The graft polymerization of styrene from the surface of fumed silica involves two steps (Scheme 1): (i) Grafting of a triethoxysilyl terminated alkoxyamine initiator (called alkoxyamine **A**) according to a procedure previously described [9], and (ii) controlled growth of polystyrene chains from the silica surface in the presence of a free alkoxyamine initiator (alkoxyamine **B**). In a typical run, the alkoxyamine **A**-functionalized silica (0.3 g), toluene (14.7 g, 0.16 mol), styrene (15.5 g, 0.15 mol), and 0.2 g (0.68 mmol) of the 'free' alkoxyamine initiator **B** corresponding to a total styrene-to-initiator molar ratio in the range 200–800 (800 in this example), were introduced in a predried Schlenk flask under an argon atmosphere. After stirring for a few minutes, the suspension was degassed by four freeze-pump-thaw cycles, and the polymerization mixture was heated to 110 °C for 22–72 h. The conversions were determined gravimetrically by precipitation in methanol. The free non-grafted polystyrene was removed from the silica suspension by successive centrifugation/redispersion cycles. The grafted polymer chains were then cleaved from the silica surface and characterized by size exclusion chromatography while the polymer grafting density was determined by thermogravimetric analysis (TGA, DuPont Instruments, heating rate: 10 °C/min) as described in our previous work [9].

2.2. Nanocomposites formation

A mixture of the PS-grafted silica particles ($M_n = 15,000$–$60,000$ g/mol) and pure polystyrene ($M_n = 100,000$ g/mol, $I_p = 1.05$) was first introduced in benzene. The blends contained 5% volume fraction of silica (silica concentration of the final grafted PS-silica/PS samples). The suspension mixture was then lyophilized and the resulting powder was stored in a vacuum oven for 1 night. The samples were compression-molded at 160 °C over 10 min. This procedure is generally better than a mechanical blending procedure at high temperature as it yields a more reproducible dispersion of the nanoparticles within the polymeric matrix.

2.3. Particle size

TEM analysis was performed on a Philips CM10 electron microscope operating at 80 kV. In a typical experiment, one drop of the colloidal dispersion was put on a carbon film supported by a copper grid and allowed to air dry before observation. Particle size was determined by DLS using a Malvern autosizer Lo-c apparatus with a detection angle of 90°. The measurements were carried at 23 °C on highly diluted samples in order to rule out interaction and multiple scattering effects. The intensity average diameter was computed from the intensity autocorrelation data using the cumulant analysis method [13].

2.4. SAXS measurements

SAXS analysis were performed at the European synchrotron radiation facility (ESRF, beam line BM2-D2AM, Grenoble, France). The use of a 2D-CCD detector (from Ropper Scientific) allowed us to record the scattering intensity in the scattering vector q-range 0.008–0.3 $Å^{-1}$. The incident energy was 16 keV and the sample-to-detector distance was close to 1 m. Silver Behenate was used as the standard for q calibration.

2.5. Viscoelastic properties

The viscoelastic properties of the nanocomposite materials were measured with a rheometrics mechanical spectrometer (RMS800). Nitrogen was used to prevent thermal oxidation. Parallel plates of diameter $\phi = 25$ mm were used as they proved to be the best suited geometry to

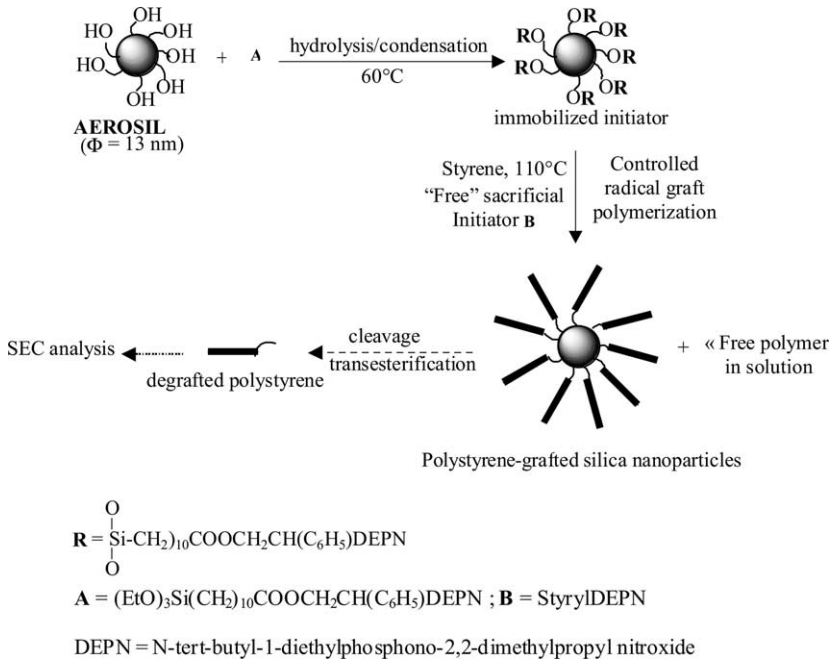

Scheme 1. Chemical route to polystyrene-decorated silica nanoparticles.

perform these experiments. The thickness of the sample (gap of the parallel-plate) was about 1 mm. The parallel-plate system was pre-heated to the temperature of the experiment. A preliminary deformation sweep experiment was first performed to determine the linear viscoelasticity deformation range. Then, frequency sweep experiments ($10^{-2} < \omega(\text{rad/s}) < 10^{2}$) were carried out in dynamic oscillatory mode at various temperatures ($T = 120$, 140, 160 and 200 °C) in order to build master curves by applying the time temperature superposition principle. All the viscoelastic data are reported in the present paper as master curves plotted at the reference temperature of $T = 160$ °C.

3. Results and discussion

3.1. Synthesis of the polystyrene-grafted silica

Contrary to other nitroxide-based systems, and particularly those using TEMPO (2′,2′,6′,6′-Tetramethyl-1′-piperidinyloxy radical) as counter radical, *N-tert*-butyl-*N*-(1-diethylphosphono-2,2-dimethylpropyl) nitroxide (DEPN)—based alkoxyamine initiators offer the advantage of providing an accurate control of molecular weights and polydispersities for a large variety of monomers including acrylates and acrylamide, and at temperatures as low as 90–110 °C, which drastically reduces the risk of thermal initiation [14]. The versatility of this system makes it particularly attractive for the elaboration of polymer layers with controlled architectures. In our synthetic strategy, an alkoxyamine based on DEPN, and carrying a terminal triethoxysilyl functional group, is first synthesized and covalently attached onto silica (Scheme 1). Polystyrene chains with controlled molecular weights and narrow polydispersities are then grown from the alkoxyamine-functionalized nanoparticles surface using a known amount of 'free' sacrificial initiator to ensure a good level of control. The chain length of the grafted polystyrene (and of the 'free' polymer) is therefore controlled by the total styrene-to-alkoxyamine molar ratio and the polymerization time. After quantitative removal of the free polymer chains by extensive washings, analysis of the recovered silica powder by FTIR and ^{13}C solid state NMR gave clear evidence of polymer grafting. The grafting density of polystyrene is determined by TGA from the weight loss and the molar mass of the grafted polymer chains after subtracting the contribution of adsorbed water and bonded initiator. As shown in our previous work, the polymer grafting density depends on the amount of grafted alkoxyamine initiator. The latter can be varied in a large range (from 0.05 to 1 μmol/m^2) by simply varying the concentration of alkoxyamine **1** introduced during grafting [9]. The characteristics of a series of PS-grafted silica samples with different grafting densities and molecular weights of the grafted polystyrene chains are listed in Table 1.

3.2. DLS measurements and TEM analysis

Insights into the composite particles size and morphology were provided by DLS measurements and TEM analysis. While the original silica particles form agglomerates and settle down in toluene, the polystyrene-grafted silica particles form stable colloidal suspensions with a mean diameter comprised between 144 and 316 nm

Table 1
Polystyrene grafting densities, molecular weights of the grafted PS chains and hydrodynamic diameters of a series of PS-grafted silica samples synthesized by NMP

Samples	1	2	3	4	5	6	7
Grafting density (μmol/m^2)	0.05	0.05	0.27	0.33	0.37	0.32	0.28
M_n of the grafted chains (g/mol)	14,800	60,000	60,000	30,900	38,700	56,000	60,000
Hydrodynamic diameter (nm)[a]	316	144	181	150	165	175	189

[a] Determined by DLS.

depending on the polymer molecular weight and grafting density (Table 1). Comparison of sample 1 and sample 2 indicates that the composite particles diameter decreases as the polystyrene chain length increases. This result shows that the dispersion ability and stability of the silica particles in toluene are significantly improved after grafting when the molecular weight of the grafted polystyrene is larger than a critical value of approximately 20,000 g/mol. Above this critical value and for a surface coverage around 0.3 μmol/m^2, the hydrodynamic diameter increases with increasing the polymer chain length (Fig. 1). This suggests that the thickness of the hairy layer surrounding the silica particles increases with increasing the molecular weight of the grafted polymer chains as expected for a controlled radical polymerization. Fig. 2 shows the TEM images of the original silica particles and of a nanocomposite sample cast from a dilute toluene suspension. The TEM micrograph of aerosil shows micrometer-sized domains of stringy-shaped aggregated particles. These agglomerates are partly destroyed after polymerization, and the silica particles appear regularly distributed within the polystyrene film. It is worth noticing that the silica beads are organized into domains which size is close to the hydrodynamic diameter determined by DLS (Table 1).

3.3. SAXS and TGA

In order to get the first morphological data about the polymer chains grafted on the silica surface, we have deduced the polymer shell thickness from TGA assuming that the polymer is distributed on the whole silica surface and considering a specific surface area of 228 m^2/g. The

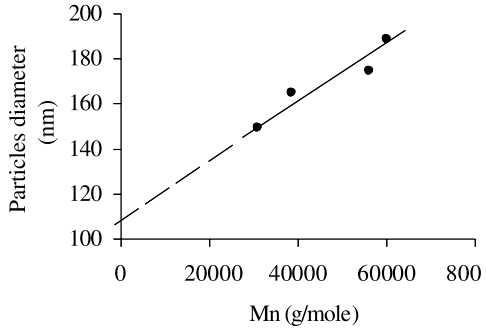

Fig. 1. Hydrodynamic diameter of the PS-grafted silica particles as a function of the molecular weight of the grafted polystyrene chains (grafting density around 0.3 μmol/m^2, see Table 1 for the exact values).

results given in Table 2 indicate a relatively low value of the corresponding interphase thickness (sample 1 and 2 with low grafting densities) which shows that the polymer chains do not distribute uniformly on the silica surface. This is in agreement with the previous DLS observations suggesting that the polymer chains distributes on the external aggregate surface rather than on individual.

The scattering curves of Fig. 3 show the evolution in a log–log plot of the scattered intensity $I(q)$ with the scattering vector $q=4\pi(\sin(\theta)/\lambda)$ (where λ is the incident wavelength, and 2θ the scattering angle) for both a polystyrene-grafted silica sample and the original aggregated silica powder (aerosil). The structure of the initial powder is complex since the Guinier and Porod regimes do not appear clearly. This is well-known to result from the aggregated structure of such systems, eventually characterised by a fractal exponent. On the contrary, surface grafting of the silica nanoparticles led to a well defined Guinier behavior:

$$I(q) = I_0 \exp\left(-\frac{R_g^2 q^2}{3}\right)$$

The coresponding gyration radius is around 170 angstrüm for surface treated silica.

At low q values below 0.01 Å^{-1}. The asymptotic behavior in the q-range 0.04 Å$^{-1} < q < 0.1$ Å^{-1} can be described by the slope α of the log–log plot, i.e. the exponent of the scaling relation:

$$I(q) = I_o q^{\alpha}$$

Table 2
Width, l_i, of the interphase layer of a series of PS-grafted silica samples characterized by SAXS and comparison with some theoretical models

Samples	1	2	3
M_n of the grafted chains (g/mol)	14,800	60,000	60,000
Grafting density (μmol/m^2)	0.05	0.05	0.27
l_i (Å)			
SAXS (l_i/α)	21/4.04	25/4.01	−/3.6
TGA	11	29	159
[a]	71	148	144
[b]	380	1480	1480

[a] Determined from the gyration radius, R_g, of a random coil using the relation: $l_i = 2\,R_g = 2[Cn(L_{c-c})^2]^{1/2}$ where C is the characteristic ratio ($C=1.89$[19]), $n=2$ DP_n and $L_{c-c}=1.54$ Å.

[b] Determined from the theoretical brush like model (extended coil) according to: $l_i = 2nL_{c-c}\sin(\theta/2)$ with $\theta=109.5°$.

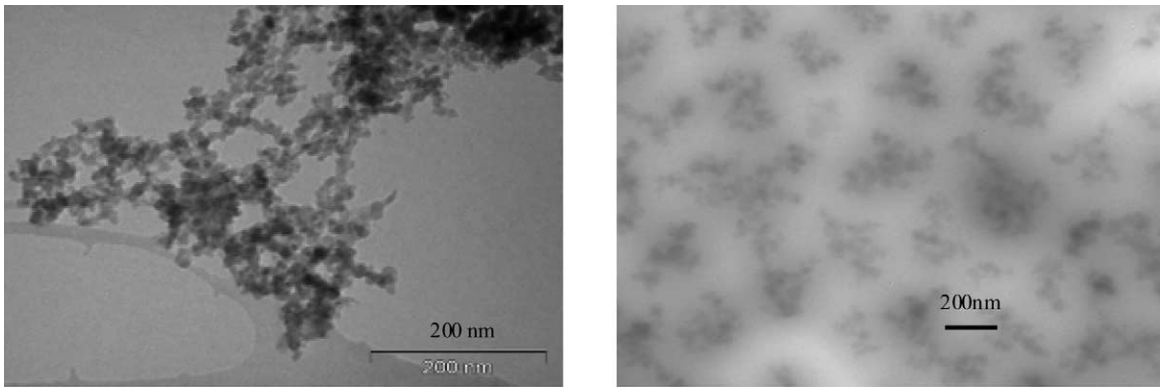

Fig. 2. TEM micrographs of (a) unmodified silica gel and (b) PS-grafted silica gel (sample 3, $M_n = 60{,}000$ g/mol).

and one of the extended Porod relation, for example:

$$I(q) = \frac{C}{q^4} - \frac{B}{q^2}$$

In principle, this behavior is evidenced in $I(q)q^2 - 1/q^2$ plots, and when B is positive, it can be used to deduce the width of the interface layer, l_i, according to [15]:

$$l_i = \sqrt{12\pi B/C}$$

The behavior of raw aerosil silica exhibits an apparent fractal exponent α close to 3.7 (Fig. 3). As a result, the value of B is large and negative, and the corresponding width of the interface layer cannot be calculated. This shows that the applicability of the method for extracting the value of l_i is limited in the case of complex aggregated structures. Nevertheless, the values of α can still be phenomenologicaly compared and related to the surface state of the filler.

As a general trend, the samples with surface-treated silica with a low grafting density exhibit an exponent slightly higher than four, thus leading to interphase widths (Table 2). The results do not compare with the real characteristic sizes of polymer chains, since the surface of silica primary particles is only partly covered, but the alteration of the aggregate structure with grafting is confirmed. Samples with high grafting density and high M_n values systematically exhibit an α value lower than 3.7. This was surprising, since a well defined and more abundant interphase could be expected in this case. We can deduce that the structural contribution of large chains attached to silica cannot be described by a gradual decrease of electron density from the silica surface to the polymer external surface. To go a step further, the scattering by Gaussian chains attached to a spherical particle is known [16] and corresponds in a first approximation to additional $1/q^2$ and constant terms in the asymptotic scattering behavior. As a result, a large apparent negative value of B (or equivalently, an α exponent that can be lower than that of raw silica) could be related with the Gaussian polymer nature of the interface.

The polystyrene thickness can also be compared to the theoretical treatment of the unperturbed radius of gyration for polystyrene [17] (Table 2). The unperturbed radius of gyration (R_g) is a characteristic dimension of molecular coils for polymer chains of high degree of polymerization (DP_n). The polystyrene shell thickness (l_i) is then expressed as follows: $l_i = 2\,R_g = 2[C_\infty n(L_{c-c})^2]^{1/2}$, where C is the characteristic ratio ($C = 1.89$ for polystyrene), $n = 2\,DP_n$ and

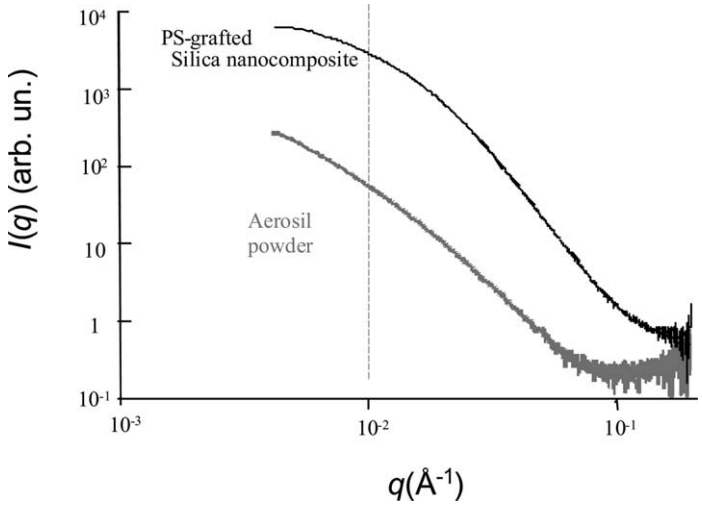

Fig. 3. Scattering diagrams of the aerosil and the PS-grafted silica powders (grafting density = 0.1 μmol/m^2, M_n of the PS-grafted chains = 20,000 g/mol).

L_{c-c} = 1.54 Å [17]. In the case of sample 3, polymer chains are presumably perturbed (and partly extended) so that the shell thickness measured by TGA is higher than the theoretical value. The estimation of the gyration radius for sample 1 and sample 2 leads to values much higher than the interface layer determined by TGA. We assume that TGA results are lower-estimated because the shell thickness is calculated from the specific area of a primary particle (228 m^2/g). However, polymer chains distributes on aggregates.

3.4. Viscoelastic behavior

The theoretical understanding of the viscoelastic behavior of filled polymers in the linear and non-linear regimes has been extensively treated in the field of elastomers [18,19]. It is generally admitted that the viscoselastic properties of rubber materials and the filler morphology (structure, particle size) are strongly related. Due to their small size and their high specific surface area, silica fillers are subjected to self aggregation, and can consequently easily form a network of connected or interacting particles in the molten polymer matrix. For example, Fig. 4 shows that nanocomposites made up of un-modified silica particles do not show any terminal flow zone: The elastic character of this suspension becomes predominant at low frequencies with the appearance of a secondary plateau ($G_0 \approx 3 \times 10^4$ Pa). The existence of a plateau in the low frequency region is clearly related to the density and strength of a network structure formed by Van Der Waals or H-bonding interactions between the filler particles, which silica network can be visualized on the TEM pictures of Fig. 2. Such a behavior was already reported by Cassagnau [20] who studied the dependence of silica particle concentrations on elastic effects. Depending on the concentration of the filler particles, floculation of the particles or clusters also leads to a filler network.

By grafting polystyrene chains onto silica, there is a breakdown of the silica–silica particles interactions because the grafted polystyrene chains induce a steric repulsion between them. Indeed, Fig. 5 shows that by grafting for example 0.05 μmol/m^2 of PS chains (M_n = 60,000 g/mol, sample 2), the elastic behavior of the suspension considerably decreases the secondary elastic plateau ($G_0 \approx 3 \times 10^3$ Pa), even if the molecular weight of the grafted PS chains stays well above the critical molecular weight entanglement of polystyrene (M_e = 18,000 g/mol). These results suggest a decrease of the size of the silica aggregates for PS-grafted silica in comparison to pure silica. In addition, Fig. 6 shows that the surface density of the grafted polymer chains also plays a major role on the viscoslastic behavior of the nanocomposites. In the present case, the grafting density (0.27 μmol/m^2, M_n = 60,000 g/mol) is about twenty times higher than that of sample 2 in Fig. 5. The 'gel' behavior disappears as, in the low frequency range, G' no longer exhibits a plateau and the macromolecular flow occurs. These results clearly show that steric repulsion between silica particles is directly influenced by the grafting density of the PS chain on the silica surface. However, this conclusion seems to contradict the simulation of Dagreou [11] which stated that increasing steric repulsions lead to a more pronounced gel behavior. Actually, the nature of silica used in their work (e.g. colloïdal silica) is quite different from the nature of the present fumed silica. Our present findings suggest that the effect of steric repulsion on the spatial organization and desagglomeration of the silica particles is more pronounced when the latter are originally aggregated than when there are naturally well dispersed. As far as fumed silica is concerned, the original silica network structure at the origin of the elastic behavior of the nanocomposite materials breaks down with steric repulsion. The multiscale fractal structure of the silica aggregates thus disappears with increasing the polymer grafting density.

Regarding now the influence of the grafted chain length on the viscoelastic behavior, Fig. 7 shows that even a small amount (0.05 μmol/m^2 (sample 1)) of short chains (M_n =

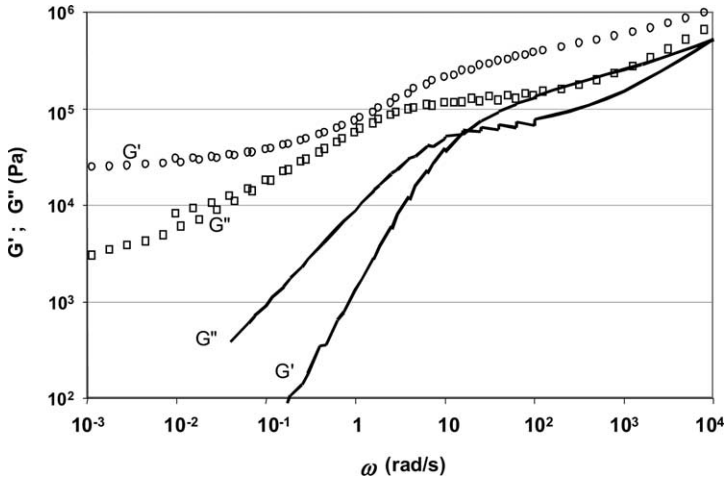

Fig. 4. Complex shear modulus versus frequency: Master curves (T_{ref} = 160 °C). Bare silica (○G′, □G″) and polystyrene matrix (–).

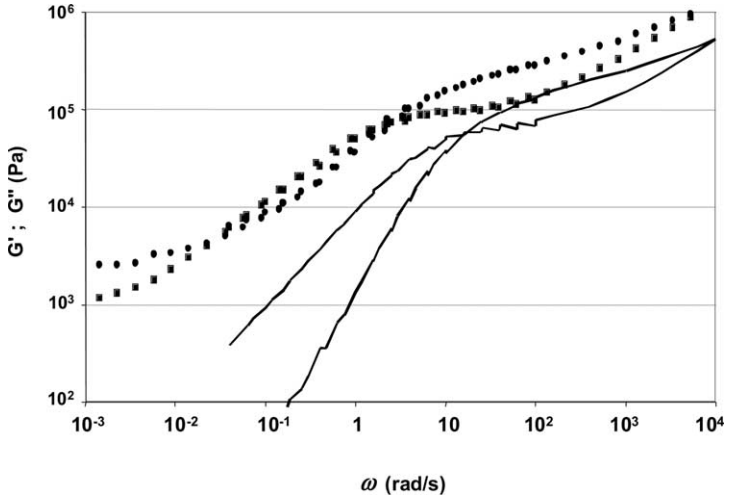

Fig. 5. Complex shear modulus versus frequency: Master curves (T_{ref} = 160 °C). PS-grafted silica (●G′, ■G″) (sample 2, M_n = 60,000 g/mol, grafting density = 0.05 μmol/m^2) and polystyrene matrix (–).

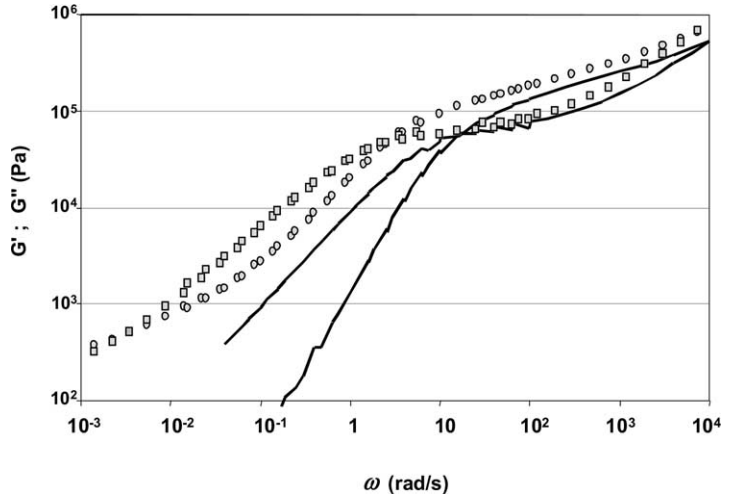

Fig. 6. Complex shear modulus versus frequency: Master curves (T_{ref} = 160 °C). PS-grafted silica (▫G′, ▫G″) (sample 3, M_n = 60,000 g/mol, grafting density = 0.27 μmol/m^2) and polystyrene matrix (–).

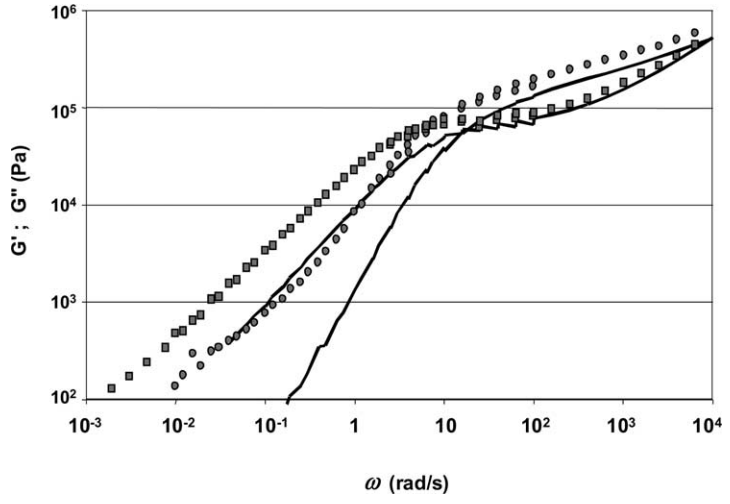

Fig. 7. Complex shear modulus versus frequency: Master curves (T_{ref} = 160 °C). PS-grafted silica (▫G′, ▫G″) (sample 1, M_n = 14,800 g/mol, grafting density = 0.05 μmol/m^2) and polystyrene matrix (–).

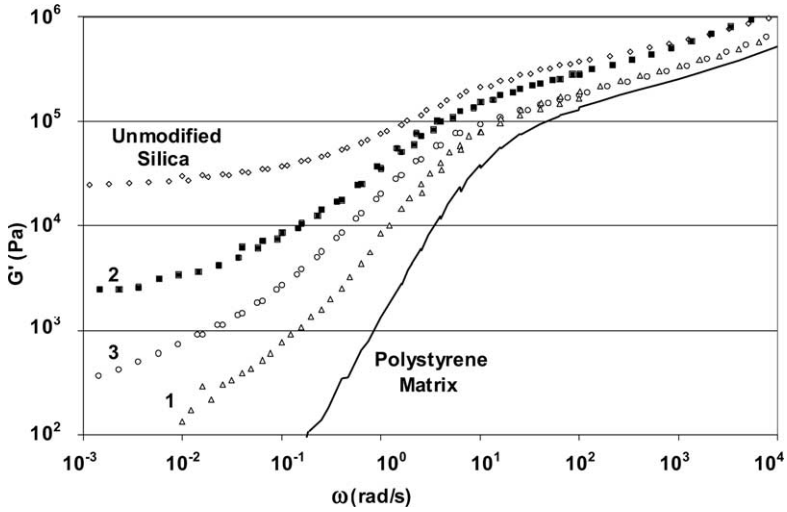

Fig. 8. Storage shear modulus of blends of polystyrene and PS-grafted silica (samples 1–3 in Table 1).

14,800 g/mol) with a molecular weight lower than the molecular weight required for physical entanglements is effective to avoid the gel effect, and also results in a fine dispersion of silica particles, although a tiny relaxation process could be present in the lower frequency range of the viscoelastic behavior. Consequently, it can be again concluded that the gel effect is not due to interactions between the polymer and the particles involving entanglements of the grafted chains in the PS matrix, but originates rather from steric repulsions between the silica particles or aggregates as a result of their tailor-made surface. To summarize the combined effects of the length and the grafting density of the PS chains, the storage shear modulus versus frequency curves of samples 1–3 are compared in Fig. 8. Although, samples 1 and 2 have the same grafting density (0.05 μmol/m^2), a different viscoelastic behavior can be observed evidencing that the length of the grafted chains plays a major role in the viscoelastic properties, shorter chains being more efficient than longer ones in avoiding formation of a silica network. As mentioned previously, the flow behavior originates from steric repulsion between silica particles within an aggregate as a result of their tailor-made surface. However, when the grafting involves long chains higher that the critical molecular weight, the entanglement of these grafted polymer chains with the free polymer (PS matrix) contributes to considerably increase the relaxation times of the terminal zone and leads to the promotion of gel behavior compared with short PS-grafted chains. Nevertheless, the high grafting density of long chains contributes to preserve the cluster structure of fumed silica that is not broken out at the same level as for short non entangled chains. Actually, two physical phenomena compete from a dynamic molecular point of view: The first one concerns the breakdown of silica aggregate clusters and the second one concerns the modification of the relaxation times of PS chains.

4. Conclusion

Polystyrene chains with molecular weights comprised between 15,000 and 60,000 g/mol and narrow polydispersities ($I_p = 1.2$) were successfully grown from the surface of silica nanoparticles. SAXS and TEM measurements were carried out to evidence the influence of grafting on the change in filler dispersion and nanostructure. Rheological measurements suggest that the grafted polymer chains on the silica particles surface create a steric repulsion between the filler particles that prevent the formation of a silica network within the polymer matrix. Further studies are underway to extrapolate this approach to colloidal silica suspensions in order to examine more precisely the influence of the polymer chain length on the thickness and structure of the polymer layer. The possibility to control nanoparticles ordering, interparticles distance, and spatial organization of the inorganic particles by varying the polymer molecular weight will also be evaluated in this future work.

References

[1] Devaux C, Beyou E, Chapel JP, Chaumont P. Eur Phys J 2002;7:345.
[2] von Werne T, Patten TE. J Am Chem Soc 1999;121(32):7409.
[3] von Werne T, Patten TE. J Am Chem Soc 2001;123(31):7497.
[4] von Werne T, Suehiro IM, Farmer S, Patten TE. Polym Mater Sci Eng 2000;82:294.
[5] Perruchot C, Khan MA, Kamitisi A, Armes SP, von Werne T, Patten TE. Langmuir 2001;17:4479.
[6] Boettcher H, Hallensleben ML, Wurm XX. Polymer Bull 2000;44:223.
[7] Parvole J, Billon L, Montfort JP. Polym Int 2002;51:1111.
[8] Kasseh A, Ait-Kadi A, Riedl B, Pierson JF. Polymer 2003;44:1367.
[9] Bartholome C, Beyou E, Bourgeat-Lami E, Chaumont P. Macromolecules 2003;36:7946.
[10] Blomberg S, Ostberg S, Harth E, Bosman AW, van Horn B, Hawker CJ. J Polym Sci, Part A Polym Chem 2002;40:1309.

[11] Dagréou S, Kasseh K, Allal A, Martin G, Ait-Kadi A. Can J Chem Eng 2002;80:1126.
[12] Sarvestani AS, Picu CR. Polymer 2004;45:7779.
[13] Koppel DJ. Chem Phys 1972;57:4814.
[14] Moad G, Solomon DH. The chemistry of free radical polymerization. New York: Elsevier Science Inc.; 1995.
[15] Glatter O, Kratky O. In: Glatter O, Kratky O, editors. Small angle X-ray scattering. London: Academic Press; 1982.
[16] Pedersen JS. Adv Colloid Interface Sci 1997;l70:171.
[17] Ma H, Wu J, Xu J. Eur Polym J 1997;33:1813.
[18] Heinrich G, Klüppel M. Adv Polym Sci 2002;160:1.
[19] Chabert E, Bornet M, Bourgeat-Lami E, Cavaillé J-Y, Dendievel R, Gauthier C, et al. Mater Sci Eng 2004;381:320.
[20] Cassagnau P. Polymer 2003;44:2455.